PLANT SCIENCES

# SHAGGY-like kinase 12 regulates flowering through mediating CONSTANS stability in *Arabidopsis*

**Ying Chen[1,2,3], Shiyong Song[2,3], Yinbo Gan[3], Lixi Jiang[3], Hao Yu[1,2]*, Lisha Shen[1]***



**Photoperiod is a major environmental cue that determines the floral transition from vegetative to reproductive development in flowering plants. *Arabidopsis thaliana* responds to photoperiodic signals mainly through a central regulator CONSTANS (CO). Although it has been suggested that phosphorylation of CO contributes to its role in photoperiodic control of flowering, how this is regulated so far remains unknown. Here, we report that a glycogen synthase kinase-3 member, SHAGGY-like kinase 12 (SK12), plays an important role in preventing precocious flowering through phosphorylating CO. Loss of function of *SK12* causes early flowering. *SK12* expression in seedlings is decreased during the floral transition, and its expression in vascular tissues is required for repressing flowering. SK12 interacts with and phosphorylates CO at threonine 119, thus facilitating CO degradation. Our findings suggest that site-specific phosphorylation of CO by SK12 is critical for modulating the photoperiodic output for the floral induction in *Arabidopsis*.**

## INTRODUCTION

The transition from vegetative to reproductive growth, namely, the floral transition, is one of the major phase changes during the plant life cycle. To tightly control the floral transition, plants have evolved complex regulatory mechanisms in response to environmental signals, such as photoperiod and temperature. In *Arabidopsis*, photoperiod relays the signals to *CONSTANS* (*CO*), which encodes a B-box zinc finger transcription factor (*1*, *2*). *CO* is strongly expressed in the vascular tissue of leaves, and its expression under the *SUCROSE TRANSPORTER 2* (*SUC2*) phloem-specific promoter is sufficient to trigger flowering (*3*, *4*). CO directly activates the expression of *FLOWERING LOCUS T* (*FT*) in the leaf veins (*5*). FT protein is then transported from leaves to the shoot apical meristem (SAM), where it interacts with FD to activate the floral meristem identity gene, *APETALA1* (*AP1*), to initiate flower development (*6*–*10*).

Regulation of *CO* transcription is mediated by multiple upstream regulators to enable its timely activation of *FT* in response to changes in photoperiod. Under long-day conditions (LDs), *CO* mRNA expression displays a diurnal oscillation with two peaks at the late afternoon and night (*11*). Precise timing of *CO* expression depends on the synchronized rhythms of *FLAVIN-BINDING*, *KELCH REPEAT*, *F-BOX 1* (*FKF1*), and *GIGANTEA* (*GI*) to form the FKF1-GI protein complex in a blue light–dependent manner to target the *CO* repressors known as CYCLING DOF FACTOR (CDF) proteins for degradation in the proteasome (*11*–*14*). The relief of *CO* repression by CDFs allows *CO* expression with a peak in the late afternoon and subsequent CO protein accumulation in the light and activation of *FT* expression. *CO* expression is promoted by FLOWERING BHLHs (FBH1–4) through their direct association with the *CO* chromatin (*15*). Under short days (SDs), the difference in the peak time of FKF1 and GI proteins results in low accumulation of the FKF1-GI complex in the afternoon, resulting in the continuous repression of CDF proteins on the *CO* promoter and thus low abundance of *CO* transcripts under light (*13*).

Previous studies have also shown that CO protein stability is modulated by various interacting partners. CO protein is degraded by the complex of the E3 ubiquitin ligase CONSTITUTIVE PHOTOMORPHOGENIC 1 (COP1) and SUPPRESSOR OF PHYA-105 (SPA) during the night (*16*, *17*). Two photoreceptors, cryptochrome 1 (CRY1) and CRY2, use different mechanisms to suppress the activity of the COP1-SPA complex to stabilize CO in a blue light–dependent manner (*18*–*20*). FKF1 also directly interacts with CO protein to facilitate CO stabilization in response to blue light (*14*). In addition, both phytochrome B (PHYB) (*17*, *21*) and another RING finger E3 ligase, HIGH EXPRESSION OF OSMOTICALLY RESPONSIVE GENES 1 (HOS1) (*22*, *23*), are involved in destabilizing CO in the early morning. These findings demonstrate that CO protein accumulation is tightly regulated under different light conditions.

Phosphorylation is one of the most common protein modifications that affect the activity or stability of transcription factors involved in various developmental processes and signaling pathways. In plants, SNF1-related protein kinase 2 (SnRK2) phosphorylates abscisic acid (ABA)–responsive element–binding factors to promote downstream ABA signaling (*24*). Phosphorylation of PHYTOCHROME-INTERACTING factor 4 (PIF4) by BRASSINOSTEROID INSENSITIVE 2 (BIN2) marks this bHLH transcription factor for proteasome degradation (*25*). Casein kinase1 proteins CK1.3 and 1.4 phosphorylate CRY2 and negatively regulates CRY2 stability (*26*). Although it has been recently shown that the phosphorylated CO protein is prone to be degraded by COP1 (*27*), the kinase(s) responsible for CO phosphorylation has not yet been characterized. Therefore, uncovering the mystery of how CO is phosphorylated will shed light on the fine-tuned control of CO abundance.

In this study, we report that a glycogen synthase kinase-3 (GSK3) member, SHAGGY-like kinase 12 (SK12), represses flowering through phosphorylating CO and negatively affecting CO protein stability in *Arabidopsis*. Loss of function of *SK12* exhibits an early-flowering phenotype. SK12 interacts with and phosphorylates CO at a specific site in vitro and in vivo, thus promoting CO degradation. Our results provide direct evidence to demonstrate an important role of

[1]Temasek Life Sciences Laboratory, National University of Singapore, Singapore 117604, Singapore. [2]Department of Biological Sciences, Faculty of Science, National University of Singapore, Singapore 117543, Singapore. [3]State Key Laboratory of Rice Biology, Zhejiang Provincial Key Laboratory of Crop Genetic Resources, Institute of Crop Science, Zhejiang University, Hangzhou 310058, China.
*Corresponding author. Email: dbsyuhao@nus.edu.sg (H.Y.); lisha@tll.org.sg (L.S.)

SK12 in mediating site-specific phosphorylation of CO for preventing precocious flowering during the floral transition.

## RESULTS

### Loss of function of *SK12* accelerates flowering in *Arabidopsis*

To identify new CO-interacting partners that are potentially involved in modulating CO function, we performed coimmunoprecipitation (CoIP) assay followed by liquid chromatography–tandem mass spectrometry (LC-MS/MS) to isolate proteins that were associated with FLAG-CO in a *co-1 FLAG-gCO* tagging line, which was generated by transforming *co-1* with the *FLAG-gCO* construct harboring the *CO* genomic region, including the 1.9-kb 5′ upstream sequence, the 1.4-kb coding sequence fused with a FLAG tag immediately after ATG, and the 0.9-kb downstream sequence. Most of the *co-1 FLAG-gCO* transformants displayed similar flowering time to wild-type plants (fig. S1A), implying that the FLAG-CO fusion protein is biologically functional. Among the independent lines generated, one representative line (#4) that contained only one transfer DNA insertion locus based on the segregation ratio was selected for further investigation. We immunoprecipitated FLAG-CO complex in nuclear protein extracts from *co-1 FLAG-gCO* (#4) leaves and identified four peptides corresponding to SK12 as a potential interacting protein of CO by the subsequent LC-MS/MS analysis (table S1 and fig. S1B). SK12 contains a typical serine/threonine (Ser/Thr) kinase domain and belongs to the subgroup I of GSK3-like kinases in *Arabidopsis* (*28*, *29*). Sequence comparison revealed that SK12 was highly conserved in different plant species and other eukaryotes, including yeast (*Saccharomyces cerevisiae*), zebrafish (*Danio rerio*), mouse (*Mus musculus*), and human (*Homo sapiens*) (fig. S2).

To explore the biological roles of *SK12*, we examined the phenotype of *sk12* (CS332559) (Fig. 1A) (*30*), where the full-length *SK12* transcript was undetectable (Fig. 1B), under different day-length conditions. *sk12* showed earlier flowering than wild-type plants under both LDs and SDs (Fig. 1, C and D). To verify whether the early-flowering phenotype of *sk12* under LDs is caused by loss of *SK12* function, we transformed *sk12* with a genomic construct (*gSK12*) harboring a 4.3-kb *SK12* genomic region, including the 1.9-kb upstream sequence, the 2.2-kb full coding sequence and introns, and the 0.2-kb 3′ untranslated region. Most of the *sk12 gSK12* T1 transformants exhibited comparable flowering time to wild-type plants, demonstrating that *SK12* is responsible for the early-flowering phenotype of *sk12* (Fig. 1E).

To confirm that *SK12* functions in the control of flowering time, we also generated the *SK12* knockdown transgenic plants by artificial microRNA (AmiR) interference (*31*). We created 20 *AmiR-sk12* transgenic lines that expressed an AmiR specifically targeting the second exon of *SK12* (Fig. 1A), among which 16 lines displayed different degrees of early flowering under LDs. We measured *SK12* expression in six selected lines and found that the degrees of early flowering were closely related to the levels of down-regulation of *SK12* transcripts (Fig. 1F), whereas the expression of the two closest homologs of *SK12*, *SK11* and *SK13*, was not obviously changed in these lines (fig. S3, A and B). These observations indicate that *SK12* represses flowering in a dosage-dependent manner. The strongest line, *AmiR-sk12* #9, displayed a comparable early-flowering phenotype to *sk12* (Fig. 1, C and D). In addition, flowering was delayed to varying degrees in transgenic plants overexpressing *SK12*, which was also correlated with increased levels of *SK12* in these lines (fig. S3, C and D). Together, these results substantiate that *SK12* represses flowering in *Arabidopsis*.

### *SK12* functions in leaf vascular tissues to repress flowering

*SK12* was ubiquitously expressed in different wild-type tissues examined with the highest expression in rosette leaves (Fig. 2A) (*30*). To check the detailed expression pattern of *SK12*, we created a *gSK12:* β-*glucuronidase* (*GUS*) reporter construct, in which the *SK12* genomic fragment used for the gene complementation assay was fused to the *GUS* gene (Fig. 1E). Among 15 independent *gSK12:GUS* lines determined, 12 lines displayed similar staining patterns. We chose one representative line for further analyses. GUS signals were found in cotyledons, rosette leaves, and vegetative shoot apices of *gSK12:GUS* plants at 5 days after germination (D5) and D11 with an overall stronger intensity at D5 (Fig. 2B). To precisely determine the temporal transcriptional levels of *SK12* in young seedlings, time-course expression of *SK12* was examined from D3 to D17 under LDs. The results revealed that its expression was gradually decreased during the floral transition and remained at low levels afterward (Fig. 2C), which is consistent with the role of *SK12* as a flowering repressor. To investigate the effect of spatial expression of *SK12* on flowering time, we transformed *sk12* with the construct in which the *SK12* coding sequence was driven by the promoter of either *SUC2* or *KNOTTED-LIKE FROM ARABIDOPSIS THALIANA 1* (*KNAT1*), which is specifically expressed either in phloem companion cells (*32*) or SAMs (*3*), respectively. Most *sk12 SUC2:SK12* T1 transformants exhibited comparable flowering time to wild type, whereas most *sk12 KNAT1:SK12* T1 transformants exhibited early flowering like *sk12* plants (Fig. 2D). These results suggest that *SK12* expression in leaf vascular tissues is required for repressing flowering.

To investigate how *SK12* regulates flowering in response to endogenous and developmental signals, we further tested *SK12* expression in various flowering mutants and under different environmental conditions. *SK12* expression was affected by the gibberellin (GA), vernalization, and autonomous and photoperiod pathways (fig. S4, A to E). In particular, *SK12* expression displayed a diurnal oscillation under LDs (fig. S4B). *SK12* expression was decreased from zeitgeber time (ZT) 4 and reached the trough at ZT12. It increased afterward and peaked at ZT20 (fig. S4B). However, *sk12* showed a comparable flowering response at 16° and 27°C to wild-type plants, indicating that *SK12* is not directly influenced in the thermosensory pathway (fig. S4F).

We further examined the subcellular localization of SK12 through transiently expressing *35S:SK12-RFP* in *Nicotiana benthamiana* leaf epidermal cells and found that SK12-RFP (red fluorescent protein) was localized in both cytoplasm and nucleus (Fig. 2E). Similar localization was also observed in *Arabidopsis* mesophyll protoplasts expressing SK12-GFP (green fluorescent protein) (Fig. 2F), indicating that SK12 may exert functions in both cytoplasm and nucleus.

### SK12 interacts with CO

As SK12 was isolated as a potential interacting partner of CO, we carried out detailed analyses of their physical interaction. First, we compared the subcellular localization of SK12 and CO in *N. benthamiana* leaf epidermal cells. Transient expression of *35S:SK12-RFP* and *35S:CO-GFP* in tobacco leaves revealed colocalization of SK12-RFP and CO-GFP in the nucleus, but not in the cytoplasm (Fig. 3A), implying that SK12 may modulate CO function in the nucleus.

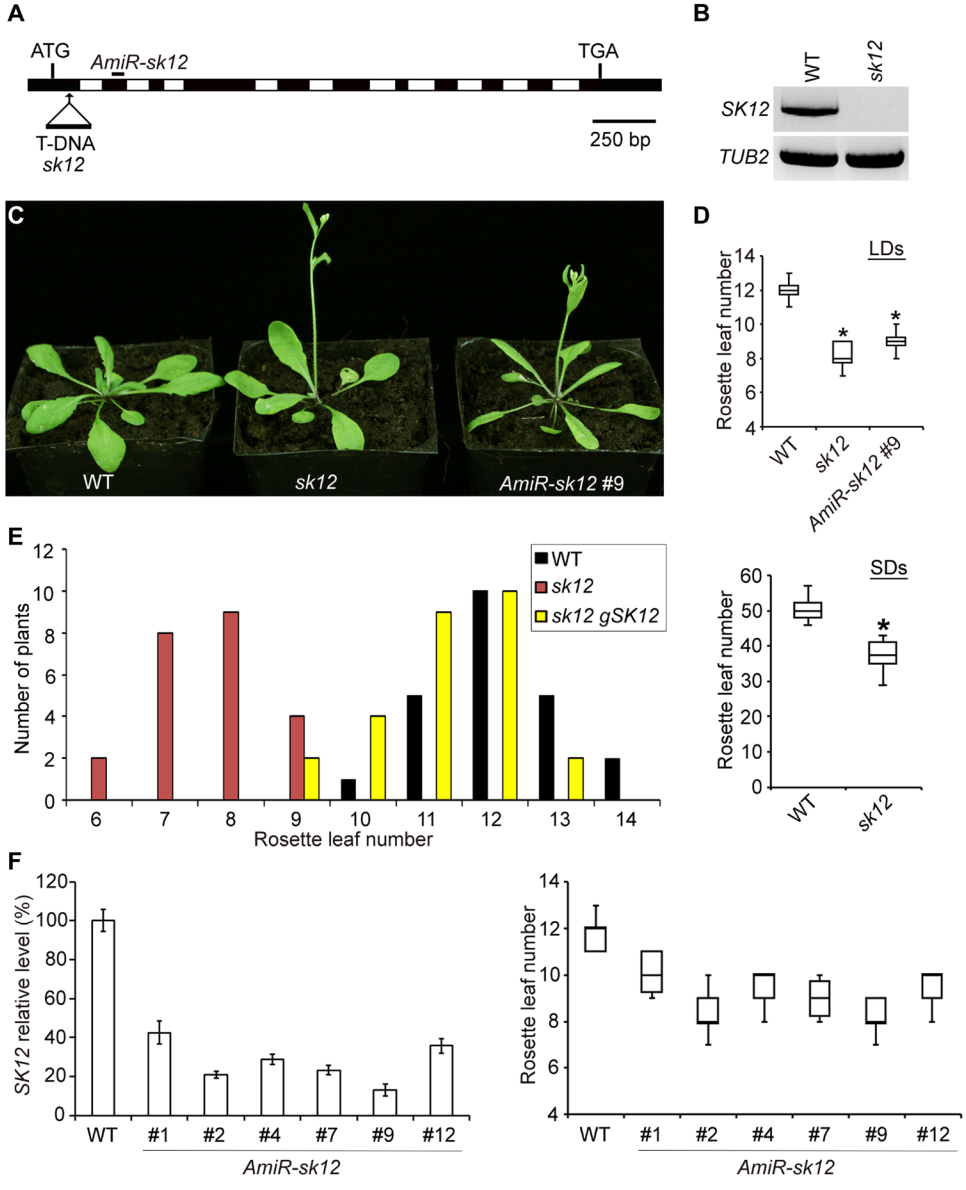


**Fig. 1. *SK12* regulates flowering time.** (**A**) Schematic diagram shows the transfer DNA (T-DNA) insertion site in *sk12* and the target site of the AmiR in *AmiR-sk12*. Black boxes, exons; white boxes, introns. (**B**) Full-length *SK12* transcript is undetectable in *sk12*. *TUB2* was the internal control. (**C**) *sk12* and *AmiR-sk12* flower early under LDs. (**D**) Flowering time of *sk12* and *AmiR-sk12* under LDs (top) and SDs (bottom). Values were scored from 20 plants of each genotype. Asterisks indicate significant differences in flowering time of *sk12* and *AmiR-sk12* compared to that of wild-type (WT) plants (two-tailed paired Student's *t* test, $P < 0.001$). (**E**) Distribution of flowering time in T1 transformants carrying *gSK12* in *sk12* background. (**F**) *SK12* down-regulation in independent *35S:AmiR-sk12* plants correlates to the degree of early flowering. *SK12* expression (left) was determined by quantitative real-time polymerase chain reaction (PCR) in 9-day-old plants under LDs at zeitgeber time (ZT) 12. *SK12* expression levels normalized to *TUB2* expression are shown relative to its level in wild-type plants set as 100%. Error bars, means ± SD; $n = 3$. The right panel shows corresponding flowering time of various plants. Values were scored from 15 plants of each genotype. Photo credit: (C) Ying Chen, National University of Singapore.

Second, in vitro glutathione *S*-transferase (GST) pull-down assay demonstrated that in vitro–translated myc-SK12 bound to GST-CO, but not GST (Fig. 3B). Furthermore, bimolecular fluorescence complementation (BiFC) experiments revealed the enhanced yellow fluorescent protein (EYFP) in the nuclei of *N. benthamiana* leaf epidermal cells, suggesting a direct interaction between SK12 and CO in living plant cells (Fig. 3C). CoIP assay using *sk12 gSK12-4HA* and *sk12 gSK12-4HA co-1 FLAG-gCO* seedlings confirmed the in vivo interaction of CO and SK12 in *Arabidopsis* (Fig. 3D). Together, these results suggest that SK12 interacts with CO in the nucleus. We further explored the genetic relationship between *sk12* and *co*. The early-flowering phenotype of *sk12* was completely suppressed by *co-1* (Fig. 3E), implying that *SK12* modulates flowering through *CO* activity. In addition, *sk12* did not further enhance the early flowering of *SUC2:CO-6HA* (Fig. 3E), which is possibly due to the high levels of *CO* expression in *SUC2:CO-6HA* (*33*).

## Phosphorylation of CO at Thr$^{119}$ is essential for CO function

The results showing SK12 interaction with CO and their effects on flowering time prompted us to examine whether CO serves as a

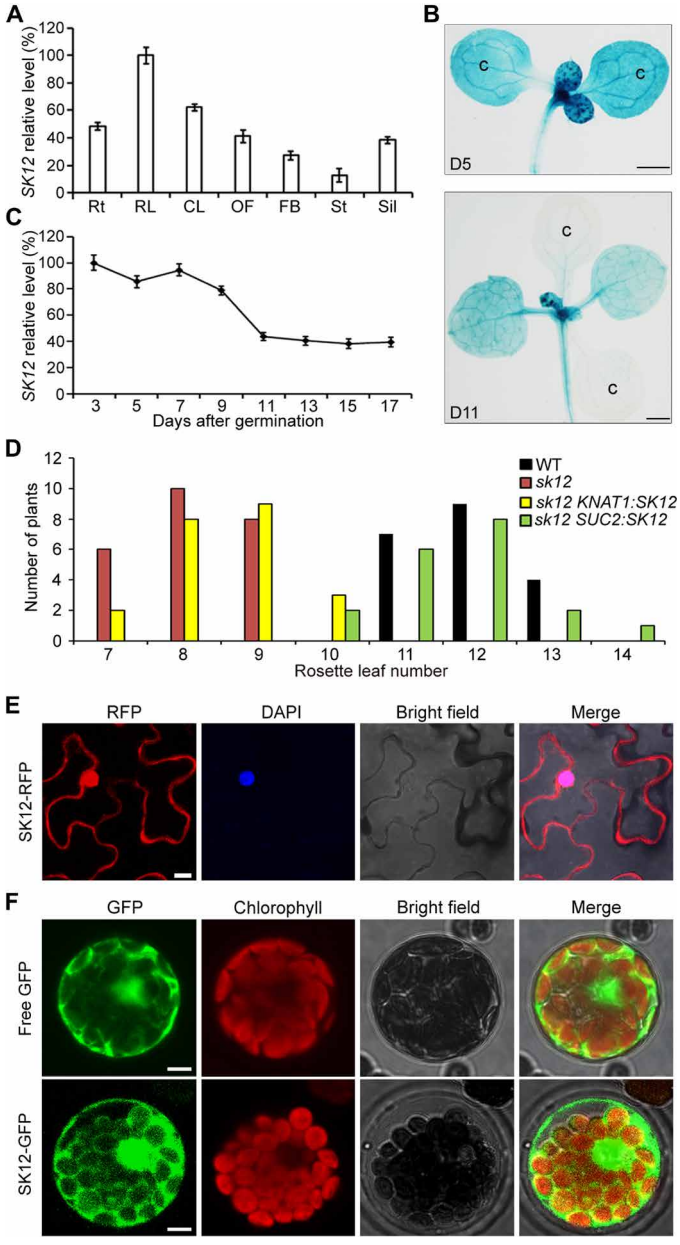


**Fig. 2. Expression pattern and subcellular localization of *SK12*.** (**A**) *SK12* expression in various tissues. Aerial tissues and roots were collected from 40-day-old wild type grown on soil and 9-day-old seedlings grown on Murashige and Skoog medium, respectively. The maximal expression of *SK12* was set as 100%. Rt, roots; RL, rosette leaves; CL, cauline leaves; OF, open flowers; FB, flower buds; St, stems; Sil, siliques. Error bars, means ± SD; $n = 3$. (**B**) GUS staining shows *SK12* expression in a 5-day-old seedling (top) and an 11-day-old seedling (bottom). c, cotyledons. Scale bars, 1 mm. (**C**) Temporal expression of *SK12* determined by quantitative real-time PCR. Wild-type plants were collected from D3 to D17 at 2-day intervals at ZT12 under LDs. The maximal expression of *SK12* was set as 100%. Error bars, means ± SD; $n = 3$. (**D**) Distribution of flowering time in T1 transgenic plants carrying *SUC2:SK12* or *KNAT1:SK12* in *sk12* background. (**E**) SK12-RFP localization in *N. benthamiana* leaf. RFP, RFP fluorescence; DAPI, fluorescence of 4′,6-diamino-2-phenylindole; merge, merge of RFP, DAPI, and bright-field images. Scale bar, 10 μm. (**F**) SK12-GFP localization of in *Arabidopsis* protoplasts. GFP, GFP fluorescence; merge, merge of GFP, chlorophyll, and bright-field images. Scale bars, 20 μm.

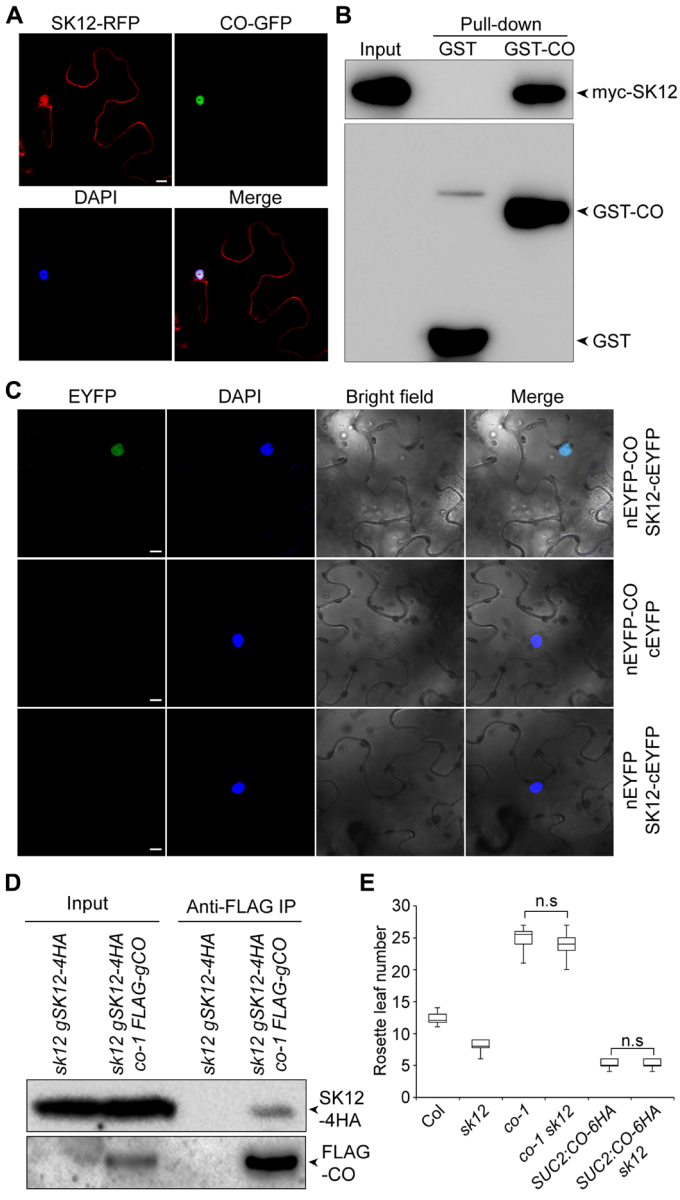


**Fig. 3. SK12 interacts with CO.** (**A**) Colocalization of SK12-RFP and CO-GFP in *N. benthamiana* leaf epidermal cells. Merge, merge of RFP, GFP, and DAPI images. Scale bar, 10 μm. (**B**) In vitro GST pull-down assay with CO and SK12. myc-tagged SK12 protein generated by in vitro translation was incubated with immobilized GST or GST-CO, respectively. Immunoblot analysis was performed using anti-myc (top) or anti-GST (bottom) antibody. Input, 5% of the in vitro translation product. (**C**) BiFC analysis of the interaction between CO and SK12. CO and SK12 were fused to nEYFP and cEYFP to generate nEYFP-CO and SK12-cEYFP, respectively. A vector containing only nEYFP or cEYFP was used as a control. EYFP, fluorescence of enhanced yellow fluorescent protein; merge, merge of EYFP, DAPI, and bright-field images. Scale bars, 10 μm. (**D**) In vivo interaction between CO and SK12 shown by CoIP. Nuclear extracts from 9-day-old *sk12 gSK12-4HA* and *sk12 gSK12-4HA co-1 FLAG-gCO* plants were incubated with anti-FLAG agarose. The input and coimmunoprecipitated protein were detected by anti-HA (top) and anti-FLAG (bottom) antibodies. (**E**) Flowering time of *co-1 sk12* and *SUC2:CO-6HA sk12*.Values were scored from 20 plants of each genotype. No significant difference (n.s.) is found between indicated genotypes (two-tailed paired Student's *t* test, $P > 0.05$).

substrate of SK12. To this end, we conducted the in vitro kinase assays using the purified maltose-binding protein (MBP)–SK12 and GST-CO fusion proteins and found that there was a mobility shift of GST-CO by MBP-SK12 in the phosphate affinity SDS–polyacrylamide gel electrophoresis (PAGE) (Fig. 4A). This shift was substantially reduced when calf intestinal alkaline phosphatase (CIAP) was added, indicating that the shift corresponds to the phosphorylated GST-CO (Fig. 4A). This result suggests that SK12 could phosphorylate CO in vitro. Furthermore, we also observed a mobility shift of phosphorylated FLAG-CO from nuclear protein extracts of *co-1 FLAG-gCO* seedlings using Phos-tag SDS-PAGE. Phosphorylated FLAG-CO was barely detected in nuclear protein extracts of *co-1 FLAG-gCO* in the *sk12* background but clearly detectable in the *sk12 gSK12-4HA* background (Fig. 4B). These results demonstrate that SK12 is essential and sufficient for phosphorylation of CO in vivo.

To identify specific phosphorylation sites on CO mediated by SK12, we analyzed the phosphorylated GST-CO products from the in vitro kinase assay by LC-MS/MS and found three potential phosphorylation sites, including Thr (T)119, T280, and T284 (fig. S5A). All these three amino acids are located in the short consensus motifs, (S/T)-X-X-X-(S/T) (S/T corresponds to Ser or Thr, and X denotes any other residue), recognized by both plant and animal GSK3 kinases (*34*). Computational analyses (www.cbs.dtu.dk/services/NetPhosK and https://scansite4.mit.edu/4.0/#scanProtein) revealed that the three sites identified by LC-MS/MS were also predicted as the potential SK12 target sites on CO. These three sites were then point-mutated to alanine (A) for an in vitro kinase assay. Only the single mutation of T119 to alanine (A) almost completely abolished in vitro phosphorylation of GST-CO by MBP-SK12 (Fig. 4C), implying that T119 targeted by SK12 is essential for phosphorylation of CO.

To explore the effects of CO phosphorylation on flowering time, we transformed *co-1* with a dephosphorylation-mimicking construct, *FLAG-gCO*$^{T119A}$, and a phosphorylation-mimicking construct, *FLAG-gCO*$^{T119D}$, in which T119 was mutated to alanine (A) or aspartic acid (D), respectively, in the *FLAG-gCO* genomic fragment that was able

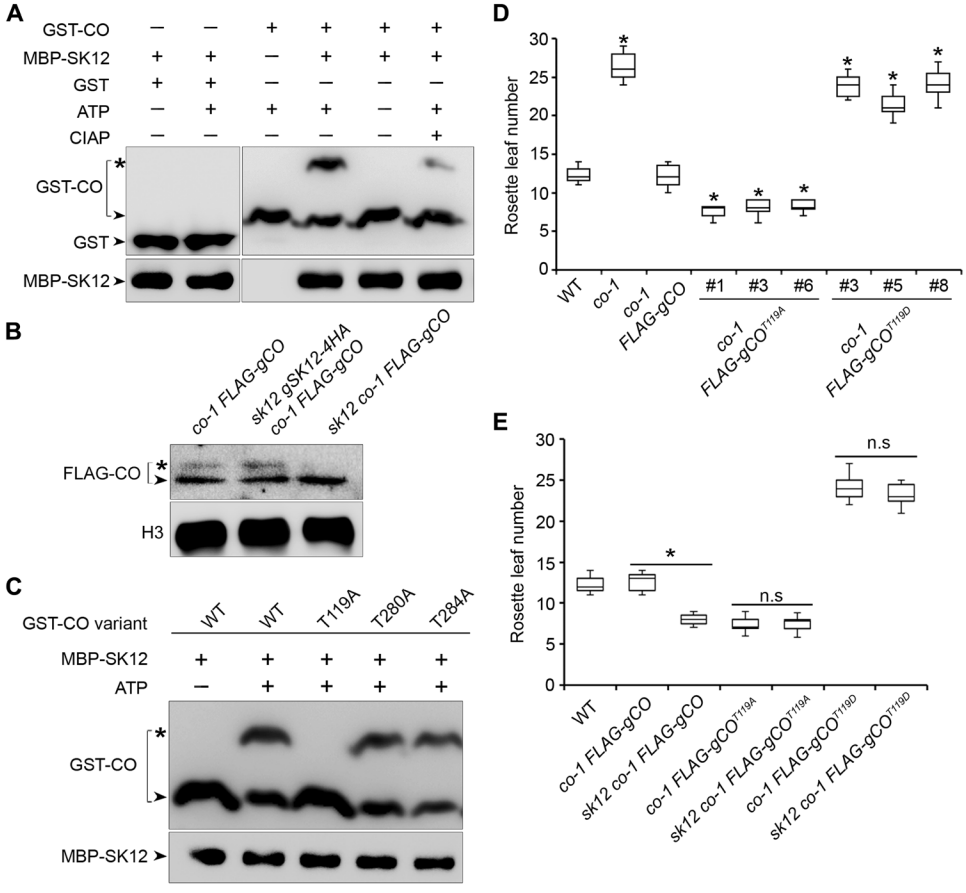


**Fig. 4. SK12 phosphorylates CO mainly through Thr$^{119}$.** (**A**) SK12 phosphorylates CO in vitro. Phosphorylation of CO and MBP-SK12 were detected by immunoblotting on Phos-tag–containing gels using anti-GST antibody (top) and regular SDS-PAGE using anti-MBP antibody (lower panel), respectively. Arrowheads and asterisks in (A) to (C) indicate unphosphorylated and phosphorylated protein forms, respectively. (**B**) Phosphorylation of CO was greatly reduced in *sk12*. Nuclear extracts were analyzed by immunoblotting on Phos-tag–containing gel using anti-FLAG antibody (top) or on regular SDS-PAGE using anti-H3 antibody (bottom). The samples were collected at ZT12. (**C**) In vitro kinase assay of wild-type and mutated GST-CO by MBP-SK12. CO proteins and MBP-SK12 were examined by immunoblotting on Phos-tag–containing gel using anti-GST antibody and on regular SDS-PAGE using anti-MBP antibody, respectively. (**D**) In vivo effects of mutated CO proteins on flowering time under LDs. Values in (D) and (E) were scored from 15 plants of each genotype. Asterisks indicate significant differences between indicated genotypes and wild type (two-tailed paired Student's *t* test, $P < 0.001$). (**E**) Flowering time of plants in various genetic backgrounds under LDs. Asterisk or n.s. indicates significant or no significant difference, respectively, between the specified pair of samples (two-tailed paired Student's *t* test; $^*P < 0.001$; n.s., $P > 0.05$).

to fully rescue the late flowering of *co-1* (fig. S1A). Phenotypic analyses of several independent lines revealed that *co-1 FLAG-gCO*$^{T119A}$ exhibited earlier flowering, whereas *co-1 FLAG-gCO*$^{T119D}$ displayed much later flowering than *co-1 FLAG-gCO* plants under LDs (Fig. 4D), indicating that the changes in T119-mediated CO phosphorylation greatly affect flowering time. In addition, in these *co-1 FLAG-gCO*, *co-1 FLAG-gCO*$^{T119A}$, and *co-1 FLAG-gCO*$^{T119D}$ transgenic lines, the *CO* expression levels were comparable (fig. S5B), further supporting that the observed flowering time differences of these transgenic lines are due to changes in CO phosphorylation but not *CO* mRNA levels. *co-1 FLAG-gCO*, *co-1 FLAG-gCO*$^{T119A}$ (#1), and *co-1 FLAG-gCO*$^{T119D}$ (#8) with similar *CO* diurnal oscillation patters (fig. S5C) were further crossed with *sk12* mutants. As expected, *sk12 co-1 FLAG-gCO* exhibited early flowering like *sk12* (Fig. 4E). However, loss of *SK12* function in *sk12* did not obviously influence the flowering phenotypes of *co-1 FLAG-gCO*$^{T119A}$ (#1) and *co-1 FLAG-gCO*$^{T119D}$ (#8) (Fig. 4E), suggesting that SK12 phosphorylates CO and affects flowering mainly through T119.

### Phosphorylation of CO at Thr$^{119}$ mediates CO destabilization

It has been reported that phosphorylated CO is the preferred substrate for degradation by the 26*S* proteasome via COP1 (*17*, *27*). Therefore, we hypothesized that phosphorylation of CO by SK12 may regulate CO abundance. We firstly tested whether SK12 affects *CO* transcription. *CO* mRNA expression was only slightly increased in *sk12* versus wild-type plants (fig. S6A), demonstrating a minor effect of SK12 on *CO* expression at the transcriptional level. Second, we monitored the amount of recombinant protein GST-CO in a cell-free protein degradation system with or without *N*-carbobenzyloxy-L-leucyl-L-leucyl-L-leucinal (MG132), a 26*S* proteasome inhibitor (*35*). In the absence of MG132, the degradation rate of GST-CO was much slower in *sk12* protein extracts than that in wild-type extracts, whereas in the presence of MG132, the abundance of GST-CO was comparable in the extracts of wild type and *sk12* (Fig. 5A). These results indicate that SK12 promotes degradation of CO by the 26*S* proteasome. Similarly, we evaluated the abundance of GST-CO$^{T119A}$ and GST-CO$^{T119D}$ in the cell-free protein degradation system and found that their abundance remained almost at the same levels in wild-type and *sk12* extracts with or without MG132 treatment (Fig. 5A). This suggests that the SK12-mediated phosphorylation of CO on T119 plays a role in CO destabilization.

To examine the effect of SK12 on CO abundance in planta, we analyzed the abundance of FLAG-CO, FLAG-CO$^{T119A}$, and FLAG-CO$^{T119D}$ in *co-1* and *co-1 sk12* backgrounds. The dephosphorylation-mimicking FLAG-CO$^{T119A}$ was more stabilized than FLAG-CO in *co-1*, whereas the phosphorylation-mimicking FLAG-CO$^{T119D}$ showed the reverse change in *co-1* (Fig. 5, B and C, and fig. S5D). Loss of *SK12* function increased the abundance of FLAG-CO in *co-1* but had no effect on the abundance of FLAG-CO$^{T119A}$ and FLAG-CO$^{T119D}$ (Fig. 5, B and C). We further examined the diurnal expression profiles of CO protein or its mutated forms in *co-1* and *co-1 sk12* mutants. The diurnal accumulation patterns of FLAG-CO were similar in *co-1* and *co-1 sk12* mutants, but FLAG-CO protein levels were constantly higher in *co-1 sk12* than in *co-1* throughout the day (Fig. 5, D and E). Similarly, the diurnal expression profiles of FLAG-CO$^{T119A}$ and FLAG-CO$^{T119D}$ were similar to that of FLAG-CO, and mutation in *SK12* did not affect the diurnal patterns or levels of FLAG-CO$^{T119A}$ or FLAG-CO$^{T119D}$ (Fig. 5, D and E). In addition, we also examined the temporal expression patterns of FLAG-CO, FLAG-CO$^{T119A}$, and FLAG-CO$^{T119D}$. These proteins exhibited a similar temporal expression pattern and were all gradually increased during seedling growth, even though FLAG-CO$^{T119A}$ and FLAG-CO$^{T119D}$ levels were higher and lower than those of FLAG-CO, respectively (fig. S7). Mutation in *sk12* resulted in increased protein levels of FLAG-CO at all time points examined but had no obvious effect on the protein levels of FLAG-CO$^{T119A}$ or FLAG-CO$^{T119D}$ (fig. S7). Together, these pieces of evidence substantiate that phosphorylation of CO on T119 by SK12 promotes CO degradation throughout the day and at different stages of seedling development.

### *SK12* regulates the expression of *FT* and *SOC1*

Since CO activates the expression of two floral pathway integrators, *FT* and *SOC1*, to promote flowering (*9*, *36*, *37*), we proceeded to test the effect of SK12-mediated CO phosphorylation on the expression of these two genes. As expected, both *FT* and *SOC1* expression was obviously increased in *sk12*, where CO protein levels were higher, versus wild-type seedlings from D3 to D11 (Fig. 6, A and B, and fig. S5E). On the contrary, the expression of *SVP* and *FLC*, two potent transcriptional repressors of *FT* and *SOC1*, was unchanged in *sk12* (fig. S6, B and C). Further comparison of *SOC1* expression in *sk12*, *ft-10*, and *ft-10 sk12* revealed that up-regulation of *SOC1* in *sk12* mutants was dependent on FT (Fig. 6B). To determine whether the diurnal oscillation pattern of *FT* is affected by *sk12*, we further measured *FT* expression in *sk12* every 4 hours over a 24-hour long-day cycle and found that *FT* expression was constitutively up-regulated in *sk12* mutants (fig. S5F). Moreover, the rhythmic *FT* expression was constantly up-regulated in *co-1 FLAG-gCO*$^{T119A}$ but down-regulated in *co-1 FLAG-gCO*$^{T119D}$ as compared with *co-1 FLAG-gCO* throughout the day (fig. S5, E and F), which is in line with their flowering phenotype (Fig. 4D). To understand the spatial effect of *SK12* on *FT* expression, we monitored the GUS staining patterns of *FT:GUS* (*4*) in *sk12* versus wild-type plants. Consistent with the quantitative expression results, FT:GUS staining intensity was obviously enhanced in the vasculature of *sk12* leaves (Fig. 6, C to E). Genetic analyses revealed that when overexpression of *FT* or *SOC1* was introduced into *sk12*, the resulting plants showed early phenotype like *35S:FT* or *35S:SOC1*, respectively (fig. S8). In addition, *ft-10*, but not *soc1-2*, mostly suppressed the early-flowering phenotype of *sk12* (Fig. 6F). These results, together with the observation that *co-1* fully suppressed early flowering of *sk12* (Fig. 3E), support that the increased CO abundance in *sk12* up-regulates *FT* expression, thus resulting in early flowering of *sk12*.

## DISCUSSION

Plants have evolved complicated flowering regulatory networks in response to environmental signals to ensure reproductive success under favorable conditions (*38*). In *Arabidopsis*, the photoperiod pathway modulates flowering time in response to day length via a core regulator, CO, which activates the rhythmic expression of *FT* under LDs (*4*, *37*). Multiple regulators are involved in regulating both *CO* mRNA and protein levels to create the daily profiles of CO to mediate the photoperiodic flowering response (*11*, *12*, *14*, *17*, *21*, *39*). In this study, we have revealed a molecular framework that a GSK3 family member SK12 phosphorylates CO at a specific site to promote CO degradation so as to prevent precocious *FT* expression at the vegetative phase, thus regulating flowering time in *Arabidopsis*.

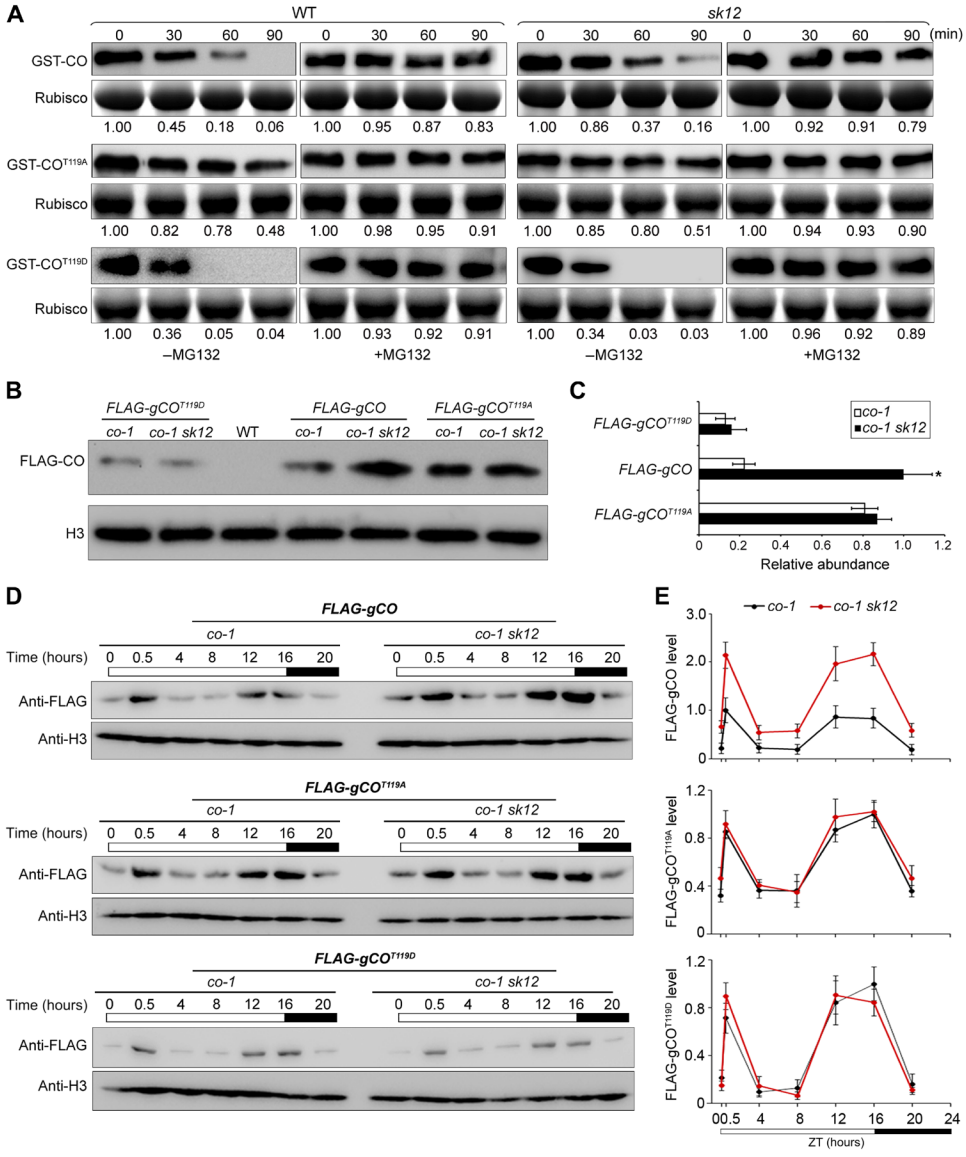


**Fig. 5. Phosphorylation on CO at Thr$^{119}$ by SK12 promotes its degradation.** (**A**) Degradation of GST-CO, GST-CO$^{T119A}$, and GST-CO$^{T119D}$ in cell-free degradation systems. Remaining CO proteins were detected by anti-GST antibody. The same amount of total extracts of wild type or *sk12* was added to each reaction, and Rubisco stained by Coomassie blue served as a loading control. Levels of protein normalized to Rubisco expression indicated below the blots are shown relative to the highest level in each type of blot set as 1.00. (**B**) Detection of FLAG-CO at ZT12 under LDs. H3 expression was used as the loading control. (**C**) Quantification of FLAG-CO levels in (B). Asterisk indicates a significant difference between wild type and *sk12* (two-tailed paired Student's *t* test, $P < 0.001$). Levels of protein normalized to H3 levels are shown relative to the highest level set as 1.0. Error bars, means ± SD; $n = 3$. (**D**) Diurnal expression patterns of CO, CO$^{T119A}$, and CO$^{T119D}$ detected by anti-FLAG antibody in *co-1* and *co-1 sk12* at D9 under LDs. H3 expression was used as loading controls. (**E**) Quantification of FLAG-CO levels in (D). Levels of protein normalized to H3 levels are shown relative to the highest level in *co-1* background set as 1.0. Error bars, means ± SD; $n = 3$.

Our results have shown that the kinase SK12 interacts with CO and specifically phosphorylates it at T119, therefore modulating CO protein abundance, as the phosphorylated form of CO is preferentially degraded by the 26*S* proteasome. This subsequently affects *FT* expression and contributes to conferring an appropriate timing of the floral transition (Fig. 6H). These findings establish *SK12* as a novel flowering time regulator that plays an important role in post-translational modification of CO. Loss of function or knockdown of *SK12* accelerates flowering (Fig. 1), whereas overexpression of *SK12* results in late flowering (fig. S3D). Although *SK12* is highly expressed throughout the aerial part of developing seedlings (Fig. 2B), its function in repressing flowering is mainly contributed by its activity in leaf vasculature tissues as *SUC2:SK12* rescue the early-flowering phenotype of *sk12* (Fig. 2D). This is in agreement with its function in interacting with and phosphorylating CO, which also functions in leaf vascular tissues to promote flowering (*4*). The phosphorylated form of FLAG-CO is greatly reduced in *sk12* mutants (Fig. 4B), indicating a critical role of SK12 in phosphorylating CO. Consistently, FLAG-CO accumulates to higher levels in *sk12* (Fig. 5, B and C). These observations, together with the genetic analysis showing the epistatic effects of *co-1* on *sk12*, suggest that the function of SK12 in mediating flowering time is mainly dependent on CO. Furthermore,

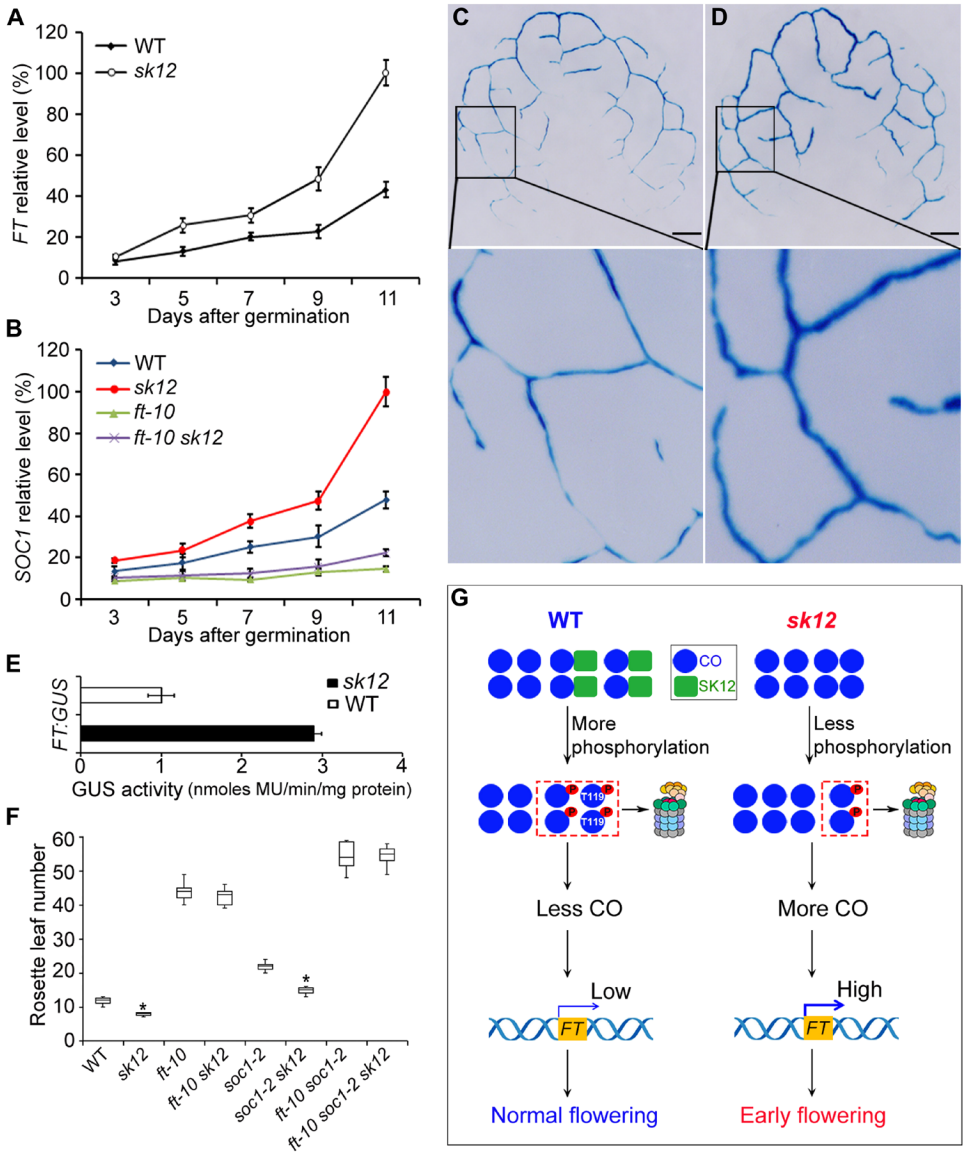


**Fig. 6. *SK12* regulates the expression of *FT* and *SOC1*.** (**A**) Temporal expression of *FT* in developing *sk12* and wild-type seedlings under LDs. All samples in (A) and (B) were collected at the end of LDs (ZT16). Gene expression levels determined by quantitative real-time PCR in (A) and (B) were normalized to *TUB2* expression and shown as relative values to the maximal gene expression level set at 100%. Error bars, means ± SD; $n = 3$. (**B**) Temporal expression of *SOC1* in developing *sk12*, *ft-10*, *ft-10 sk12*, and wild-type seedlings under LDs. (**C** and **D**) *GUS* staining of true leaves in 11-day-old long-day-grown *FT:GUS* (C) and *sk12 FT:GUS* (D) plants. The bottom panels show higher magnification of the areas indicated in the upper panels. Scale bars, 1 mm. (**E**) Quantitative comparison of GUS activity in wild type and *sk12*. Error bars, means ± SD; $n = 3$. (**F**) Flowering time of various mutants grown under LDs. Values were scored from 15 plants of each genotype. Asterisks indicate significant difference in flowering time between wild type and *sk12* as well as between *soc1-2* and *soc1-2 sk12* (two-tailed paired Student's *t* test, $P < 0.001$). (**G**) A model describing regulation of flowering time by site-specific phosphorylation of CO mediated by SK12. *SK12* is highly expressed at the vegetative phase and specifically phosphorylates CO at T119, which promotes CO degradation at the vegetative stage, thus precisely controlling the timing of floral transition in *Arabidopsis*.

the diurnal oscillation expression pattern of *SK12* under LDs indicates that *SK12* is regulated by the photoperiod pathway (fig. S4B). *SK12* expression is decreased from ZT4 and reaches the trough at ZT12 when CO protein is highly accumulated (*13*, *14*). *SK12* expression increases afterward and peaks at ZT20 when CO is degraded by COP1 (*17*). The opposite expression patterns of *SK12* mRNA and CO protein are in line with our model that phosphorylation of CO by SK12 promotes CO degradation. Hence, it would be interesting to further explore the mechanism by which the photoperiod pathway modulates *SK12* expression.

We have demonstrated that SK12 phosphorylates CO specifically at T119, which is located in THHQS, a typical consensus motif recognized by GSK3s (*34*). The phosphorylation-mimicking mutant FLAG-gCO$^{T119D}$ and dephosphorylation-mimicking mutant FLAG-gCO$^{T119A}$ of FLAG-gCO have opposite roles in affecting flowering time (Fig. 4D) and CO protein stability (Fig. 5, B and C). CO protein is degraded by the COP1-SPA E3 ubiquitin ligase complex at night (*16*, *17*). In the early morning, CO degradation requires the activities of red light photoreceptor PHYB (*17*, *21*) and another ubiquitin ligase HOS1 (*22*, *23*). Phosphorylated form of CO is not only the

preferential target of COP1 for degradation as the phosphorylated CO is more abundant in *cop1* mutant, but also the preferred substrate of red light–induced proteolysis (*27*). Our findings have revealed that phosphorylation of CO at T119 by SK12 negatively affects CO protein abundance, indicating that SK12 could be an important regulator involved in modulating CO protein levels under various light conditions. Since phosphorylation might affect CO stability by different ways, such as altering its interaction with COP1 or with FKF1 that stabilizes CO protein in response to blue light (*14*), it will be interesting to further explore these possibilities using CO and its phosphorylation-mimicking mutant $CO^{T119D}$ or dephosphorylation-mimicking mutant $CO^{T119A}$ to understand the regulatory effects of phosphorylation of CO by SK12.

In addition to SK12-mediated phosphorylation at T119 of CO, we envisage that CO phosphorylation could involve other regulators and sites. First, a previous study has shown that the CCT domain of CO protein ($CO^{298\text{-}373}$) contains CO phosphorylation sites as phosphorylation of CO-CCT-YFP has been detected in *35S:CO-CCT-YFP* transgenic lines (*27*). This suggests that, in addition to the T119 site that is specifically phosphorylated by SK12 revealed in our study, there could be other phosphorylation sites in the CCT domain of CO. Notably, the CCT domain of CO is phosphorylated but is insufficient to cause degradation (*27*). In contrast, phosphorylation of CO at T119 is closely related with CO protein degradation and abundance, indicating that phosphorylation of CO at different sites may have different effects on CO protein stability or activity. Second, there may be other kinases that act to phosphorylate CO. The possible candidates include the close homologs of SK12 in the GSK3 family, such as SK11 and SK13. Since our recent study has shown that SK12 and SK11 function redundantly in seed development (*30*), whether SK11 also acts together with SK12 in controlling the floral transition needs to be further investigated.

*SK12* is expressed in almost all the plant tissues (Fig. 2A) (*30*). In addition to its role in regulating the floral transition, *SK12* is highly expressed in seeds where it phosphorylates TRANSPARENT TESTA GLABRA1 (TTG1) to mediate carbon partitioning in seeds (*30*). Expression of *SK12* in floral organ primordia is also associated with its role in controlling floral organ formation, since knockdown lines of *SK11* and *SK12* display pleotropic floral phenotypes, including an increased number of petals and sepals and alteration of gynoecium patterning (*28*). In addition, *SK12* has also been reported to suppress the expression levels of *C-REPEAT/DRE BINDING FACTORs* (*CBFs*) and *RESPONSIVE TO DESICCATION 29A* (*RD29A*) to negatively regulate freezing response (*40*). Despite the above progress in understanding multiple biological roles of SK12 in plants, their substrates involved in plant development or plant responses to environmental signals are still largely unknown. Further investigation of the interacting partners of SK12 and the effects of their interaction on different developmental processes will provide more insights into the regulatory mechanisms underlying which GSK3 family kinases contribute to plant development.

## MATERIALS AND METHODS

### Plant materials and growth conditions

*Arabidopsis thaliana* ecotypes Col and Landsberg *erecta* (L*er*) were grown on soil or Murashige and Skoog plates under LDs (16-hour light/8-hour dark) or SDs (8-hour light/16-hour dark) at 23° ± 2°C. The mutants *sk12*, *co-1*, *gi-1*, *ft-10*, *soc1-2*, *fve-4*, and *svp-41* are in Col background, while *fca-1*, *fpa-1*, and *ga1-3* are in L*er* background (*30*, *41*–*43*). All transgenic plants were generated in the Col background through *Agrobacterium tumefaciens*–mediated transformation and selected by Basta on soil.

### Plasmid construction

For the complementation test, a 4.3-kb *SK12* genomic fragment (*gSK12*), including a 1.9-kb upstream sequence, a 2.2-kb coding sequence and introns, and a 0.2-kb 3′ untranslated region, was amplified using primers gSK12-F-Eco RI and gSK12-R-*Xba*I. The resulting polymerase chain reaction (PCR) fragment was digested and cloned into pHY105 (*44*). To construct *gSK12-4HA*, the *SK12* genomic fragment, including 1.9-kb upstream sequence and 2.2-kb coding sequence and introns, was amplified with primers gSK12-F-Eco RI and gSK12-R-*Xma*I and cloned into pGreen-4HA to obtain an in-frame fusion of SK12-4HA. The pGreen-6HA vector was cut with Bam HI and self-ligated to generate pGreen-4HA (*41*). To construct *gSK12:GUS*, the *SK12* genomic region was amplified with primers gSK12-F-Eco RI and gSK12-R-*Xma*I and cloned into pHY107 (*44*). To construct *AmiR-sk12*, design of the AmiR was performed using the software on the website (http://wmd3.weigelworld.org). On the basis of the *SK12* sequence, a set of four primers was generated and used for the PCR amplification according to the published protocol (*31*). The resulting products were digested with Eco RI and Bam HI and cloned into pGreen-35S. To construct *35S:SK12*, *35S:SK12-GFP*, and *35S:SK12-RFP*, the *SK12* coding region was amplified and cloned into pGreen-35S, pGreen-35S-GFP, and pGreen-35S-RFP, respectively, using In-Fusion HD cloning (Clontech) following the manufacturer's instructions. The coding regions of GFP and RFP were cloned into pGreen-35S to generate pGreen-35S-GFP and pGreen-35S-RFP, respectively.

To construct *FLAG-gCO*, a 4.2-kb genomic fragment of *CO* was divided into the 1.9-kb upstream sequence (*gCO*-1) and the 2.3-kb CO coding sequence (*gCO*-2). The sequence of *FLAG* fused to *CO* after its start codon was included in the forward primer for amplifying *gCO*-2. *gCO*-1 and *gCO*-2 fragments were amplified and cloned into the pENTR vector (*45*). On the basis of this construct, *FLAG-gCO*$^{T119A}$ and *FLAG-gCO*$^{T119D}$ were generated by QuikChange Site-Directed Mutagenesis. Recombination of the DNA fragment from the entry clones to pBGW by LR reaction was performed according to the manufacturer's instructions (Invitrogen). Primer sequences for plasmid construction are listed in table S2.

### Expression analysis

Total RNA was extracted using the RNeasy Plant Mini Kit (Qiagen) and reverse-transcribed with the SuperScript III First-Strand Synthesis System (Invitrogen) according to the manufacturer's instructions. Gene-specific primers for quantitative real-time PCR were designed by the QuantPrime tool (www.quantprime.de/), and the specificity of each primer pair was determined by its dissociation curve. The complementary DNAs (cDNAs) were mixed together with primers and SYBR Green PCR Master Mix (Applied Biosystems) in the reactions following the manufacturer's instructions. Quantitative real-time PCR was performed using three biological replicates with three technical replicates each on the 7900HT Fast Real-Time PCR System (Applied Biosystems). *TUB2* was used as an internal control. The relative expression levels were determined as previously described (*41*). Briefly, the difference between the cycle threshold (Ct) of target genes and the Ct of *TUB2* ($\Delta Ct = Ct_{target\ gene} - Ct_{TUB2}$) was

used to obtain the normalized expression of target genes. Primers used for gene expression analysis are listed in table S2.

For *gSK12:GUS* reporter construct, we checked 15 independent transgenic lines at the T3 generation and selected one representative line for further analysis. Tissues for GUS staining were first infiltrated with staining solution [50 mM sodium phosphate buffer (pH 7.0), 0.5 mM potassium ferrocyanide, 0.5 mM potassium ferricyanide, and X-Gluc (0.5 mg/ml)] in a vacuum chamber and subsequently incubated with the same solution at 37°C for 6 hours. Samples were dehydrated through an ethanol series and finally photographed under a microscope.

### CoIP and LC-MS/MS analysis

Nine-day-old seedlings of *co-1 FLAG-gCO* and wild type were collected at ZT12 and ground into fine powder in liquid nitrogen. The nuclear protein was isolated as previously described (*46*). Nuclear isolation buffer [0.25 M sucrose, 15 mM PIPES (pH 6.8), 5 mM $MgCl_2$, 60 mM KCl, 15 mM NaCl, 1 mM $CaCl_2$, and 0.9% Triton X-100] with freshly added 1 mM phenylmethylsulfonyl fluoride (PMSF) and 1× protease inhibitor cocktail (Roche) was added to each sample to resuspend the plant tissues. The homogenate was filtered and centrifuged at 4000 rpm for 10 min at 4°C. The pellets were resuspended in the nuclei isolation buffer, followed by the same centrifugation as the previous step. After centrifugation, the pellets were resuspended in nuclei lysis buffer [50 mM Hepes (pH 7.5), 150 mM NaCl, 1 mM EDTA, 1% SDS, 0.1% Na deoxycholate, and 1% Triton X-100] with freshly added 1 mM PMSF and 1× protease inhibitor cocktail and kept on ice for 10 min. After centrifugation at the highest speed for 5 min, the supernatant was collected and incubated with anti-FLAG M2 agarose beads (Sigma-Aldrich) for 4 hours at 4°C. After washing, the immunoprecipitated protein mixture was eluted and analyzed by LC-MS/MS using a TripleTOF 5600 System (AB Sciex, Protein and Proteomics Centre in the National University of Singapore). The spectrum data were searched against the TAIR10 database using Protein Prospector. The peptides with confidence less than 95% were removed. Part of the peptides from the LC-MS/MS analysis of two biological replicates of *co-1 FLAG-gCO* versus wild type were listed in table S1.

For CoIP to verify the in vivo interaction of CO and SK12, *sk12 gSK12-4HA* and *co-1 FLAG-gCO sk12 gSK12-4HA* seedlings were harvested, and nuclear proteins were extracted as described above, followed by incubation with anti-FLAG M2 agarose (Sigma-Aldrich). The immunoprecipitated proteins and the protein extracts as inputs were resolved by SDS-PAGE and detected by anti-HA (hemagglutinin) antibody (Santa Cruz Biotechnology).

### In vitro GST pull-down assay

The coding region of *CO* was cloned into *pGEX-6p-2* vector (Pharmacia, USA) using In-Fusion HD cloning (Clontech) following the manufacturer's instructions. The primers used for this cloning were listed in table S2. The GST-CO fusion protein was produced by *Escherichia coli* Rosetta (DE30) cells harboring the corresponding construct with 0.2 mM isopropyl β-D-1-thiogalactopyranoside (IPTG) at 16°C. The soluble GST-CO protein was extracted and immobilized on glutathione Sepharose beads (Amersham Biosciences) for subsequent pull-down assays. To produce myc-tagged SK12 protein, the full-length *SK12* cDNA was cloned into pGBKT7 (Clontech). The resulting plasmid was added to the TNT T7 Quick Coupled Transcription/Translation Systems (Promega) to synthesize myc-tagged SK12. myc-SK12 was incubated with the immobilized GST and GST-CO fusion protein. Proteins retained on the beads were resolved by SDS-PAGE and detected with anti-myc antibody (Santa Cruz Biotechnology).

### BiFC analysis

To construct *35S:nEYFP-CO*, the full-length coding region of *CO* was firstly cloned into pSAT4A-nEYFP-N1 vector (*47*) to generate pSAT4A-nEFYP-CO, and then the resulting cassette, including the nEYFP-CO fusion protein and the *35S* constitutive promoter, was cloned into the pGreen binary vector HY105. Similarly, to generate *35S:SK12-cEYFP*, *SK12* coding region was firstly cloned into pSAT4-cEYFP-C1 vector (*47*), and the resulting cassette, including the SK12-cEYFP fusion protein and *35S* promoter, was subsequently cloned into HY105. The primers for plasmid construction are listed in table S2. For the BiFC experiment, the *Agrobacteria* harboring the desired vectors were coinfiltrated into 3-week-old long-day-grown tobacco (*N. benthamiana*) leaves as previously described (*48*). The leaves were examined 2 days after infiltration under a confocal microscope.

### Transient expression of proteins in tobacco cells and *Arabidopsis* mesophyll protoplasts

*Agrobacterium* cultures with expression vectors grown overnight were harvested and resuspended with infiltration buffer [10 mM MES (pH 5.6), 10 mM $MgCl_2$, and 100 μM acetosyringone] with optical density at 600 nm at 0.5. To compare protein localization, equal volumes of infiltration solutions containing different expression vectors were mixed together and then infiltrated into the abaxial surface of 3-week-old long-day-grown tobacco (*N. benthamiana*) leaves with syringes. The leaves were examined 40 to 48 hours after infiltration under a confocal microscope.

Isolation of *Arabidopsis* protoplasts and polyethylene glycol (PEG)–mediated transfection were performed as previously described (*49*). Briefly, mesophyll protoplasts were isolated from leaves of 15-day-old *Arabidopsis* under LDs using the Tape-*Arabidopsis* Sandwich method (*47*) in enzyme solution [20 mM MES (pH 5.7), 1.5% cellulase R10, 0.4% macerozyme R10, 0.4 M mannitol, 20 mM KCl, 10 mM $CaCl_2$, and 0.1% bovine serum albumin]. The isolated protoplasts were washed twice with ice-cold W5 solution [154 mM NaCl, 125 mM $CaCl_2$, 5 mM KCl, 5 mM glucose, and 2 mM MES (pH 5.7)] and resuspended in MMg solution [0.4 M mannitol, 15 mM $MgCl_2$, and 4 mM MES (pH 5.7)]. The *35S:SK12-GFP* or *35S:GFP* plasmid was incubated with isolated protoplasts and PEG4000 solution (40% PEG, 0.1 M $CaCl_2$, and 0.2 M mannitol) for 5 min at room temperature, after which transfected protoplasts were washed and incubated in W5 solution in darkness for 12 to 16 hours before being examined under a confocal microscope.

### Phos-tag SDS-PAGE

Phos-tag SDS-PAGE was performed with protein gels containing 50 μM Phos-tag (Wako Pure Chemical Industries) and 100 μM $MnCl_2$. After electrophoresis, the Phos-tag–containing gel was washed in transfer buffer [25 mM tris-HCl, 192 mM glycine, and 20% methanol] supplemented with 10 mM EDTA three times and then washed in transfer buffer followed by blotting and detection with appropriate antibodies.

### In vitro kinase assay

The coding region of *SK12* was cloned into pMAL-C2X (New England Biolabs) using In-Fusion HD cloning (Clontech). GST-CO

or MBP-SK12 fusion proteins were produced by *E. coli* Rosetta (DE30) cells harboring the corresponding construct with 0.2 mM IPTG at 16°C. The soluble GST-CO and MBP-SK12 proteins were extracted and purified by glutathione Sepharose beads (Amersham Biosciences) and amylose resin (New England Biolabs), respectively, according to the manufacturers' instructions. The concentrations of purified GST-CO and MBP-SK12 fusion proteins were determined by Bradford assay (Bio-Rad). In vitro kinase assays were performed as described previously (*50*). The purified MBP-SK12 (2 μg) was incubated with GST-CO (2 μg) in 12 μl of kinase buffer [25 mM tris (pH 7.5), 12 mM $MgCl_2$, 1 mM dithiothreitol (DTT), and 1 mM adenosine triphosphate (ATP)] with or without CIAP at 37°C for 30 min. The reaction products were resolved by electrophoresis using 8% SDS-PAGE and Phos-tag and detected by anti-GST antibody (Santa Cruz Biotechnology). The reaction products were also analyzed by LC-MS/MS using a TripleTOF 5600 System (AB Sciex, Protein and Proteomics Centre in the National University of Singapore) to identity the specific phosphorylation site(s) on CO mediated by SK12. For detecting SK12 target sites on CO, several Thr amino acids identified by LC-MS/MS were mutated into Ala and then subjected to in vitro kinase assay under the same procedure.

### Cell-free degradation assay

Wild-type and *sk12* plants were grown at 23°C under LDs, and 9-day-old seedlings were harvested and ground to a fine powder in liquid nitrogen. Total protein was extracted using extraction buffer [25 mM tris-HCl (pH 7.4), 150 mM NaCl, 1% Nonidet P-40, 1 mM EDTA, and 5% glycerol] with freshly added 1 mM PMSF and 1× protease inhibitor cocktail. Protein concentrations were determined by the Bio-Rad protein assay (Bio-Rad). GST-CO (200 ng) or its mutated versions of recombinant proteins were incubated with 100 μl of plant extracts (containing approximately 500 μg of total proteins) of wild type or *sk12* in reaction buffer [20 mM tris-HCl (pH 7.5), 10 mM $MgCl_2$, 1 mM DTT, and 1 mM ATP] (*35*) at 37°C for 30, 60, and 90 min in the presence or absence of 50 μM MG132, respectively. SDS-PAGE analysis was conducted to determine the abundance of GST-CO. Densitometric analysis of immunoblot results was performed using ImageJ software (U.S. National Institutes of Health).

## SUPPLEMENTARY MATERIALS

Supplementary material for this article is available at http://advances.sciencemag.org/cgi/content/full/6/24/eaaw0413/DC1

View/request a protocol for this paper from *Bio-protocol*.

## REFERENCES AND NOTES


1. R. Khanna, B. Kronmiller, D. R. Maszle, G. Coupland, M. Holm, T. Mizuno, S.-H. Wu, The *Arabidopsis* B-box zinc finger family. *Plant Cell* **21**, 3416–3420 (2009).
2. J. Putterill, F. Robson, K. Lee, R. Simon, G. Coupland, The *CONSTANS* gene of arabidopsis promotes flowering and encodes a protein showing similarities to zinc finger transcription factors. *Cell* **80**, 847–857 (1995).
3. H. An, C. Roussot, P. Suárez-López, L. Corbesier, C. Vincent, M. Piñeiro, S. Hepworth, A. Mouradov, S. Justin, C. Turnbull, G. Coupland, CONSTANS acts in the phloem to regulate a systemic signal that induces photoperiodic flowering of *Arabidopsis*. *Development* **131**, 3615–3626 (2004).
4. S. Takada, K. Goto, TERMINAL FLOWER2, an Arabidopsis homolog of HETEROCHROMATIN PROTEIN1, counteracts the activation of *FLOWERING LOCUS T* by CONSTANS in the vascular tissues of leaves to regulate flowering time. *Plant Cell* **15**, 2856–2865 (2003).
5. S. B. Tiwari, Y. Shen, H. C. Chang, Y. Hou, A. Harris, S. F. Ma, M. McPartland, G. J. Hymus, L. Adam, C. Marion, A. Belachew, P. P. Repetti, T. L. Reuber, O. J. Ratcliffe, The flowering time regulator CONSTANS is recruited to the *FLOWERING LOCUS T* promoter via a unique *cis*-element. *New Phytol.* **187**, 57–66 (2010).
6. M. Abe, Y. Kobayashi, S. Yamamoto, Y. Daimon, A. Yamaguchi, Y. Ikeda, H. Ichinoki, M. Notaguchi, K. Goto, T. Araki, FD, a bZIP protein mediating signals from the floral pathway integrator FT at the shoot apex. *Science* **309**, 1052–1056 (2005).
7. M. A. Blázquez, D. Weigel, Integration of floral inductive signals in *Arabidopsis*. *Nature* **404**, 889–892 (2000).
8. L. Corbesier, C. Vincent, S. Jang, F. Fornara, Q. Fan, I. Searle, A. Giakountis, S. Farrona, L. Gissot, C. Turnbull, G. Coupland, FT protein movement contributes to long-distance signaling in floral induction of *Arabidopsis*. *Science* **316**, 1030–1033 (2007).
9. I. Kardailsky, V. K. Shukla, J. H. Ahn, N. Dagenais, S. K. Christensen, J. T. Nguyen, J. Chory, M. J. Harrison, D. Weigel, Activation tagging of the floral inducer *FT*. *Science* **286**, 1962–1965 (1999).
10. Y. Kobayashi, H. Kaya, K. Goto, M. Iwabuchi, T. Araki, A pair of related genes with antagonistic roles in mediating flowering signals. *Science* **286**, 1960–1962 (1999).
11. F. Fornara, K. C. Panigrahi, L. Gissot, N. Sauerbrunn, M. Rühl, J. A. Jarillo, G. Coupland, *Arabidopsis* DOF transcription factors act redundantly to reduce *CONSTANS* expression and are essential for a photoperiodic flowering response. *Dev. Cell* **17**, 75–86 (2009).
12. T. Imaizumi, T. F. Schultz, F. G. Harmon, L. A. Ho, S. A. Kay, FKF1 F-box protein mediates cyclic degradation of a repressor of *CONSTANS* in *Arabidopsis*. *Science* **309**, 293–297 (2005).
13. M. Sawa, D. A. Nusinow, S. A. Kay, T. Imaizumi, FKF1 and GIGANTEA complex formation is required for day-length measurement in *Arabidopsis*. *Science* **318**, 261–265 (2007).
14. Y. H. Song, R. W. Smith, B. J. To, A. J. Millar, T. Imaizumi, FKF1 conveys timing information for CONSTANS stabilization in photoperiodic flowering. *Science* **336**, 1045–1049 (2012).
15. S. Ito, Y.-H. Song, A. R. Josephson-Day, R. J. Miller, G. Breton, R. G. Olmstead, T. Imaizumi, FLOWERING BHLH transcriptional activators control expression of the photoperiodic flowering regulator *CONSTANS* in *Arabidopsis*. *Proc. Natl. Acad. Sci. U.S.A.* **109**, 3582–3587 (2012).
16. S. Laubinger, V. Marchal, J. Le Gourrierec, S. Wenkel, J. Adrian, S. Jang, C. Kulajta, H. Braun, G. Coupland, U. Hoecker, *Arabidopsis* SPA proteins regulate photoperiodic flowering and interact with the floral inducer CONSTANS to regulate its stability. *Development* **133**, 3213–3222 (2006).
17. S. Jang, V. Marchal, K. C. S. Panigrahi, S. Wenkel, W. Soppe, X.-W. Deng, F. Valverde, G. Coupland, *Arabidopsis* COP1 shapes the temporal pattern of CO accumulation conferring a photoperiodic flowering response. *EMBO J.* **27**, 1277–1288 (2008).
18. H.-L. Lian, S.-B. He, Y.-C. Zhang, D.-M. Zhu, J.-Y. Zhang, K.-P. Jia, S.-X. Sun, L. Li, H.-Q. Yang, Blue-light-dependent interaction of cryptochrome 1 with SPA1 defines a dynamic signaling mechanism. *Genes Dev.* **25**, 1023–1028 (2011).
19. B. Liu, Z. Zuo, H. Liu, X. Liu, C. Lin, *Arabidopsis* cryptochrome 1 interacts with SPA1 to suppress COP1 activity in response to blue light. *Genes Dev.* **25**, 1029–1034 (2011).
20. Z. Zuo, H. Liu, B. Liu, X. Liu, C. Lin, Blue light-dependent interaction of CRY2 with SPA1 regulates COP1 activity and floral initiation in Arabidopsis. *Curr. Biol.* **21**, 841–847 (2011).
21. F. Valverde, A. Mouradov, W. Soppe, D. Ravenscroft, A. Samach, G. Coupland, Photoreceptor regulation of CONSTANS protein in photoperiodic flowering. *Science* **303**, 1003–1006 (2004).
22. A. Lazaro, F. Valverde, M. Piñeiro, J. A. Jarillo, The *Arabidopsis* $E_3$ ubiquitin ligase HOS1 negatively regulates CONSTANS abundance in the photoperiodic control of flowering. *Plant Cell* **24**, 982–999 (2012).
23. A. Lazaro, A. Mouriz, M. Piñeiro, J. A. Jarillo, Red light-mediated degradation of CONSTANS by the $E_3$ ubiquitin ligase HOS1 regulates photoperiodic flowering in arabidopsis. *Plant Cell* **27**, 2437–2454 (2015).
24. Y. Ma, I. Szostkiewicz, A. Korte, D. Moes, Y. Yang, A. Christmann, E. Grill, Regulators of PP2C phosphatase activity function as abscisic acid sensors. *Science* **324**, 1064–1068 (2009).
25. S. Bernardo-García, M. de Lucas, C. Martínez, A. Espinosa-Ruiz, J.-M. Davière, S. Prat, BR-dependent phosphorylation modulates PIF4 transcriptional activity and shapes diurnal hypocotyl growth. *Genes Dev.* **28**, 1681–1694 (2014).
26. S.-T. Tan, C. Dai, H.-T. Liu, H.-W. Xue, *Arabidopsis* casein kinase1 proteins CK1.3 and CK1.4 phosphorylate cryptochrome2 to regulate blue light signaling. *Plant Cell* **25**, 2618–2632 (2013).
27. L. Sarid-Krebs, K. C. S. Panigrahi, F. Fornara, Y. Takahashi, R. Hayama, S. Jang, V. Tilmes, F. Valverde, G. Coupland, Phosphorylation of CONSTANS and its COP1-dependent degradation during photoperiodic flowering of Arabidopsis. *Plant J.* **84**, 451–463 (2015).
28. M. C. Dornelas, A. A. Van Lammeren, M. Kreis, Arabidopsis thaliana SHAGGY-related protein kinases (AtSK11 and 12) function in perianth and gynoecium development. *Plant J.* **21**, 419–429 (2000).
29. C. Jonak, H. Hirt, Glycogen synthase kinase 3/SHAGGY-like kinases in plants: An emerging family with novel functions. *Trends Plant Sci.* **7**, 457–461 (2002).
30. C. Li, B. Zhang, B. Chen, L. Ji, H. Yu, Site-specific phosphorylation of TRANSPARENT TESTA GLABRA1 mediates carbon partitioning in *Arabidopsis* seeds. *Nat. Commun.* **9**, 571 (2018).

31. R. Schwab, S. Ossowski, M. Riester, N. Warthmann, D. Weigel, Highly specific gene silencing by artificial microRNAs in *Arabidopsis*. *Plant Cell* **18**, 1121–1133 (2006).
32. A. Imlau, E. Truernit, N. Sauer, Cell-to-cell and long-distance trafficking of the green fluorescent protein in the phloem and symplastic unloading of the protein into sink tissues. *Plant Cell* **11**, 309–322 (1999).
33. X. Hou, J. Zhou, C. Liu, L. Liu, L. Shen, H. Yu, Nuclear factor Y-mediated H3K27me3 demethylation of the SOC1 locus orchestrates flowering responses of *Arabidopsis*. *Nat. Commun.* **5**, 4601 (2014).
34. H. Ryu, H. Cho, K. Kim, I. Hwang, Phosphorylation dependent nucleocytoplasmic shuttling of BES1 is a key regulatory event in brassinosteroid signaling. *Mol. Cells* **29**, 283–290 (2010).
35. F. Wang, D. Zhu, X. Huang, S. Li, Y. Gong, Q. Yao, X. Fu, L.-M. Fan, X. W. Deng, Biochemical insights on degradation of *Arabidopsis* DELLA proteins gained from a cell-free assay system. *Plant Cell* **21**, 2378–2390 (2009).
36. H. Lee, S.-S. Suh, E. Park, E. Cho, J. H. Ahn, S.-G. Kim, J. S. Lee, Y. M. Kwon, I. Lee, The AGAMOUS-LIKE 20 MADS domain protein integrates floral inductive pathways in *Arabidopsis*. *Genes Dev.* **14**, 2366–2376 (2000).
37. A. Samach, H. Onouchi, S. E. Gold, G. S. Ditta, Z. Schwarz-Sommer, M. F. Yanofsky, G. Coupland, Distinct roles of CONSTANS target genes in reproductive development of *Arabidopsis*. *Science* **288**, 1613–1616 (2000).
38. J. D. Salazar, T. Saithong, P. E. Brown, J. Foreman, J. C. W. Locke, K. J. Halliday, I. A. Carré, D. A. Rand, A. J. Millar, Prediction of photoperiodic regulators from quantitative gene circuit models. *Cell* **139**, 1170–1179 (2009).
39. G. Claisse, B. Charrier, M. Kreis, The *Arabidopsis thaliana* GSK3/shaggy like kinase AtSK3-2 modulates floral cell expansion. *Plant Mol. Biol.* **64**, 113–124 (2007).
40. Q. Guan, J. Wu, Y. Zhang, C. Jiang, R. Liu, C. Chai, J. Zhu, A DEAD box RNA helicase is critical for pre-mRNA splicing, cold-responsive gene regulation, and cold tolerance in *Arabidopsis*. *Plant Cell* **25**, 342–356 (2013).
41. D. Li, C. Liu, L. Shen, Y. Wu, H. Chen, M. Robertson, C. A. Helliwell, T. Ito, E. Meyerowitz, H. Yu, A repressor complex governs the integration of flowering signals in *Arabidopsis*. *Dev. Cell* **15**, 110–120 (2008).
42. P. Han, B. Garcia-Ponce, G. Fonseca-Salazar, E. R. Alvarez-Buylla, H. Yu, *AGAMOUS-LIKE* 17, a novel flowering promoter, acts in a *FT*-independent photoperiod pathway. *Plant J.* **55**, 253–265 (2008).
43. H. Yu, Y. Xu, E. L. Tan, P. P. Kumar, AGAMOUS-LIKE 24, a dosage-dependent mediator of the flowering signals. *Proc. Natl. Acad. Sci. U.S.A.* **99**, 16336–16341 (2002).
44. C. Liu, J. Zhou, K. Bracha-Drori, S. Yalovsky, T. Ito, H. Yu, Specification of *Arabidopsis* floral meristem identity by repression of flowering time genes. *Development* **134**, 1901–1910 (2007).
45. Y. Yan, L. Shen, Y. Chen, S. Bao, Z. Thong, H. Yu, A MYB-domain protein EFM mediates flowering responses to environmental cues in *Arabidopsis*. *Dev. Cell* **30**, 437–448 (2014).
46. A. Saleh, R. Alvarez-Venegas, Z. Avramova, An efficient chromatin immunoprecipitation (ChIP) protocol for studying histone modifications in *Arabidopsis* plants. *Nat. Protoc.* **3**, 1018–1025 (2008).
47. V. Citovsky, L.-Y. Lee, S. Vyas, E. Glick, M.-H. Chen, A. Vainstein, Y. Gafni, S. B. Gelvin, T. Tzfira, Subcellular localization of interacting proteins by bimolecular fluorescence complementation *in planta*. *J. Mol. Biol.* **362**, 1120–1131 (2006).
48. I. A. Sparkes, J. Runions, A. Kearns, C. Hawes, Rapid, transient expression of fluorescent fusion proteins in tobacco plants and generation of stably transformed plants. *Nat. Protoc.* **1**, 2019–2025 (2006).
49. F.-H. Wu, S.-C. Shen, L.-Y. Lee, S.-H. Lee, M.-T. Chan, C.-S. Lin, Tape-*Arabidopsis* sandwich – A simpler *Arabidopsis* protoplast isolation method. *Plant Methods* **5**, 16 (2009).
50. Y. Yin, Z.-Y. Wang, S. Mora-Garcia, J. Li, S. Yoshida, T. Asami, J. Chory, BES1 accumulates in the nucleus in response to brassinosteroids to regulate gene expression and promote stem elongation. *Cell* **109**, 181–191 (2002).


**Acknowledgments:** We thank the Arabidopsis Biological Resource Center for providing seeds. We thank the Protein and Proteomics Centre (PPC) in the Department of Biological Sciences, National University of Singapore for mass spectrometry service, and members of Shen and Yu laboratories for discussion and comments on the manuscript. **Funding:** This work was supported by Academic Research Fund (MOE2015-T2-2-002) from the Ministry of Education–Singapore, the Singapore National Research Foundation under its Competitive Research Programme (NRF2010NRF-CRP002-018), the Agency for Science, Technology and Research (A*STAR) under its Industry Alignment Fund - Pre Positioning (IAF-PP) (A19D9a0096), the National Natural Science Foundation of China (31529001), and the intramural research support from National University of Singapore and Temasek Life Sciences Laboratory. **Author contributions:** Y.C., H.Y., and L.S. conceived the project and designed the experiments. Y.C. and S.S. performed the experiments. Y.C., H.Y., and L.S. conducted all statistical analyses. Y.C., Y.G., L.J., H.Y., and L.S. analyzed the data. Y.C., H.Y., and L.S. wrote the paper. All authors read and approved of the manuscript. **Competing interests:** The authors declare that they have no competing interests. **Data and materials availability:** All data needed to evaluate the conclusions in the paper are present in the paper and/or the Supplementary Materials. Additional data related to this paper may be requested from the authors.

Submitted 14 November 2018
Resubmitted 5 September 2019
Accepted 14 April 2020
Published 12 June 2020
10.1126/sciadv.aaw0413

**Citation:** Y. Chen, S. Song, Y. Gan, L. Jiang, H. Yu, L. Shen, SHAGGY-like kinase 12 regulates flowering through mediating CONSTANS stability in *Arabidopsis*. *Sci. Adv.* **6**, eaaw0413 (2020).